Bioorganic & Medicinal Chemistry Letters 22 (2012) 3727–3731

Contents lists available at SciVerse ScienceDirect

Bioorganic & Medicinal Chemistry Letters

journal homepage: www.elsevier.com/locate/bmcl

Discovery of XL413, a potent and selective CDC7 inhibitor

Elena S. Koltun *, Amy Lew Tsuhako, David S. Brown, Naing Aay, Arlyn Arcalas, Vicky Chan, Hongwang Du, Stefan Engst, Kim Ferguson, Maurizio Franzini, Adam Galan, Charles R. Holst, Ping Huang, Brian Kane, Moon H. Kim, Jia Li, David Markby, Manisha Mohan, Kevin Noson, Arthur Plonowski, Steven J. Richards, Scott Robertson, Kenneth Shaw, Gordon Stott, Thomas J. Stout, Jenny Young, Peiwen Yu, Cristiana A. Zaharia, Wentao Zhang, Peiwen Zhou, John M. Nuss, Wei Xu, Patrick C. Kearney

Exelixis, Department of Drug Discovery, 210 East Grand, South San Francisco, CA 94080, USA

ARTICLE INFO

Article history:
Available online 16 April 2012

Keywords:
CDC7 kinase inhibitor
CK2 inhibitors
Benzofuropyrimidinone
Cell cycle arrest

ABSTRACT

CDC7 is a serine/threonine kinase that has been shown to be required for the initiation and maintenance of DNA replication. Up-regulation of CDC7 is detected in multiple tumor cell lines, with inhibition of CDC7 resulting in cell cycle arrest. In this paper, we disclose the discovery of a potent and selective CDC7 inhibitor, XL413 (**14**), which was advanced into Phase 1 clinical trials. Starting from advanced lead **3**, described in a preceding communication, we optimized the CDC7 potency and selectivity to demonstrate in vitro CDC7 dependent cell cycle arrest and in vivo tumor growth inhibition in a Colo-205 xenograft model.

CDC7 is a serine/threonine kinase that plays a critical role in the initiation of DNA synthesis and in S phase cell cycle check point control.[1] Human CDC7 phosphorylates the mini-chromosome maintenance protein (MCM2) leading to the unwinding of double-stranded DNA during the G1/S transition.[2] CDC7's role in DNA unwinding is essential for DNA replication, and subsequent cell proliferation. In fact, inhibition of CDC7 in tumor cells with small molecules or small interfering RNAs results in defective S phase progression that leads to a halt in cell cycle progression and subsequent p53-independent apoptotic cell death.[3] These results, coupled with the fact that upregulation of CDC7 has been observed in numerous tumor cell lines[4] (colon, lung, ovary, breast, leukemia, and prostate), make CDC7 an attractive target for cancer therapy. Several research groups have reported potent CDC7 inhibitors for cancer therapy.[5]

Compound **1**, **2**, and **3** all contributed to provide the direction for our investigation (Fig. 1). Compounds **1** has been identified as a result of HTS effort for multiple kinase targets. It possessed moderate inhibitory potency for three kinases: CDC7 (IC_{50} = 2.0 μM), PIM1 (IC_{50} = 0.53 μM), and CK2 (IC_{50} = 1.5 μM). Compound **2** was a potent lead compound in our CK2 inhibitor program which also had CDC7 activity (CK2 IC_{50} = 19 nM, CDC7 IC_{50} = 1.4 nM, PIM IC_{50} = 332 nM) but had poor plasma exposure in mouse PK (100 mg/kg, po: 0.82 μM, 1 h; 0.31 μM, 4 h). It was noted that the fused tricyclic benzofuropyrimidinone (BFP) system in compound **1** had a similar spatial layout as (4-hydroxy-3-methylphenyl)pyrimidinone in compound **2**. Compared to **1**, compound **2** had an additional phenyl group attached to pyrimidinone ring on the right-had side. In the preceding communication,[6] we disclosed highlights of our PIM1 program, where we combined structures **1** and **2** into a chimeric structure. Compound **3** was one of the compounds that resulted from that effort; it was a potent inhibitor for all three kinases: PIM1 (IC_{50} = 11 nM), CK2 (IC_{50} = 28 nM), CDC7 (IC_{50} = 7.7 nM) and had favorable ADME/PK property (e.g., mouse PK exposures 100 mg/kg; 101 μM, 1 h; 49 μM, 4 h). Compound **3** was also shown to be efficacious in multiple tumor xenograft models, although it was not well tolerated at high doses (data not shown). Having established that an inhibitor of three kinases (PIM1, CK2, and CDC7 all valid cancer targets individually) with good PK exposure has a significant in vivo efficacy, we focused our effort on creating a selective and more cell potent CDC7 inhibitor. The goals were to demonstrate whether CDC7 inhibition alone can inhibit or reverse tumor growth, and if a selective compound would be better tolerated.

Since access to a crystal structure of CDC7 was not feasible, a homology model[7] was built based on an in-house high resolution co-crystal[8] structure data of CK2 protein with **3** (Fig. 2). CK2 is structurally closest analog of CDC7.[5d] We also hypothesized that the two proteins were similar in ATP binding region due to parallel SAR observed in structurally related compounds. Multiple BFP analogs are potent CK2 inhibitors, which made co-crystallization with CK2 very accessible. The orientation of the BFP core in **3** docked (gray) in the CDC7 model is only slightly different from that bound (blue) in the CK2 crystal structure. Among the residues that are

* Corresponding author at present address: Numerate, Inc., 1150 Bayhill Drive, San Bruno, CA 94066, USA. Tel.: +1 6507032244, +1 (650) 472 0632.
E-mail address: elena@numerate.com (E.S. Koltun).

0960-894X/$ - see front matter © 2012 Elsevier Ltd. All rights reserved.
http://dx.doi.org/10.1016/j.bmcl.2012.04.024

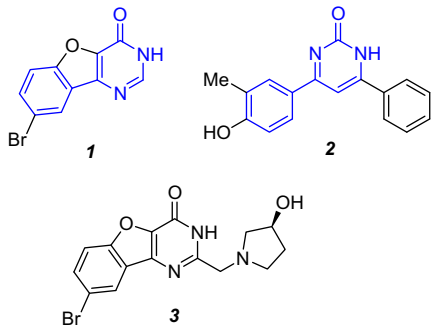

Figure 1. HTS hit **1**, PIM1 inhibitor **2**, and crossover compound **3**.

different, Pro135 (CDC7) versus Glu114 (CK2) in the kinase hinge motif is the most interesting. A conformational constraint imposed by the Pro135 backbone forces Met134 (the gatekeeper) to be positioned closer to the compound's binding site in CDC7. The phenyl portion of BFP moiety resides near the hinge motif, although the bromine is unlikely to make any specific interactions. The oxygen of the pyrimidinone forms a hydrogen bond (1.9 Å zmCK2) with the Lys of the conserved (Lys-Glu) salt bridge. The hydroxyl pyrrolidine side chain is positioned towards the G-loop and the hydroxy moiety makes a hydrogen bond (1.6 Å zmCK2) with Asn (Asn182 in CDC7, Asn161 in CK2). The comparison of the docked (CDC7) and bound (zmCK2) lead compound **3**, reveals few more different residues around the pyrrolidine binding region, Ser181 in CDC7 is different from His160 in CK2, and G-loop Glu66 in CDC7 is replaced by Arg47 in CK2.

We started by exploring the SAR on the left-hand side of the BFP core.[9] Synthesis of bis-substituted compound **9g** is shown in Scheme 1. 2-Hydroxy-4-methoxybenzonitrile was brominated to yield aldehyde **4**. The resulting bromo-aldehyde was converted to the corresponding bromo-nitrile **5** by reaction with hydroxylamine followed by $POCl_3$. Nitrile **5** was alkylated with chloroacetamide under basic conditions to give amide **6**, which underwent intramolecular cyclization to yield benzofuran **7**. Acylation with chloroacetyl chloride, followed by nucleophilic substitution with

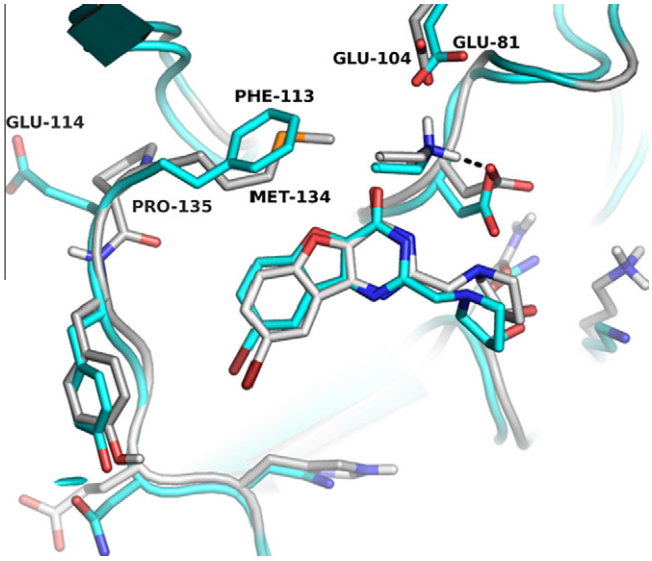

Figure 2. CDC7 homology model (gray) built using the zmCK2 X-ray crystal structure (blue) as a template (PDB code 4ANM). Compound **3** (gray) docked in the CDC7 model (gray) overlaid with **3** bound (blue) in the zmCK2 crystal structure (blue).

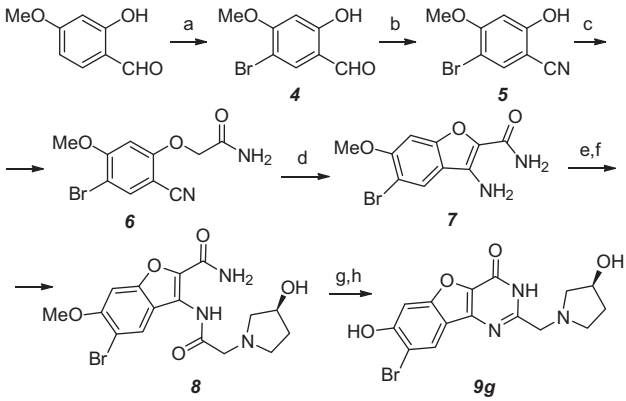

Scheme 1. Reagents and conditions: (a) Br_2, AcOH; (b) NH_2OH, followed by $POCl_3$; (c) $ClCH_2CONH_2$, K_2CO_3, DMF, 80 °C, 85%; (d) KOH, DMF, 85 °C, 95%; (e) $ClCH_2COCl$, DCE, 65 °C, 85%; (f) (*S*)-3-hydroxypyrrolidine, EtOH, 85 °C, 90%; (g) 1 M NaOH, EtOH, 85 °C, 90%; (h) BBr_3, CH_2Cl_2.

(*S*)-3-hydroxypyrrolidine gave bi-cyclic amide **8**. Cyclization under basic conditions to form the BFP core, followed by deprotection of the phenol with BBr_3 gave the desired analog **9g**. Compounds **3**, **9a–f**, **9h–i**, and **10a–f** were prepared via similar methods using either commercially available nitriles or the corresponding aldehydes. In the case of bis-amine derivatives **10b** and **10c**, *N*′-Boc-protected amines were used, and the parent compounds were obtained by deprotection with 4N HCl in dioxane.[9]

In general, only few changes to the 8-bromo substituted BFP core were tolerated (Table 1). Placing small substituents in the 6- and 9-positions resulted in a loss of CDC7 activity (**9d**, **9e**). The 7- and 8-positions were more amendable to substitutions, as analogs with a chlorine (**9b**, IC_{50} = 2.2 nM) and a methoxy group (**9c**, IC_{50} = 9.0 nM) in the 8-position were equipotent to lead compound **3**, suggesting that a chlorine or a methoxy group could be a good alternative to the bromine in the 8-position. 7-Hydroxy compound **9g** resulted in an improvement in potency compared to the lead compound **3**. We used CK2 as a surrogate, and obtained an X-ray structure with bound **9g**. We postulated that the improvement in potency came as a result of an interaction of the 7-hydroxy with the backbone C=O of the Pro135 in the hinge region of CDC7 (Fig. 2). However, compound **9g** did not show good exposure in a mouse PK study (100 mg/kg (PO): 1.4 μM at 1 h, 0.15 μM at 4 h). Docking studies showed that the left-hand side of the molecule

Table 1
SAR study in the right-hand portion of BFP[10]

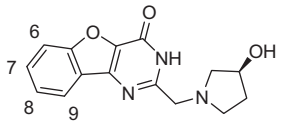

	R in position				CDC7
	6	7	8	9	IC_{50} (nM)
3	H	H	Br	H	7.7
9a	H	H	H	H	>3000
9b	H	H	Cl	H	2.2
9c	H	H	OMe	H	9.0
9d	Me	H	Br	H	1350
9e	H	H	Br	OMe	>3000
9f	H	H	$-OCH_2O-$		14
9g	H	OH	Br	H	1.0
9h	H	Me	Br	H	104
9i	H	OMe	Br	H	>3000

is packed tightly against the hinge region of the protein. This was confirmed when **9i** was synthesized, and found to be inactive.

Next, we turned our attention towards the modifications in the right-hand side hydroxyl-pyrrolidine, taking advantage of the existence of non-conserved acidic residues in this region. First, we investigated the effect of substituted N-linked pyrrolidines on CDC7 activity and selectivity against PIM1 and CK2. We examined the CDC7 potency and selectivity of BFP analogs made for the previously described PIM program,[6] and prepared over 40 additional analogs with the 8-bromo substitution on the left hand side. A select set of these analogs is presented in Table 2. Although some of these analogs showed single digit nM activity against CDC7, we were unable to find at least 10-fold selectivity among compounds with N-linked pyrrolidine derivatives **10**. Consequently, we expanded our search to C-linked heterocycles and acyclic substituent containing a basic amino group, as replacements for the hydroxyl-pyrrolidine.

The synthesis of C-linked analogs **13b** and **13g** is shown in Scheme 2. The 8-bromobenzofuran intermediate **11** was prepared via methods described in Scheme 1, and coupled with activated *N*-Boc-proline to yield intermediate **12**. Boc deprotection with 4N HCl in dioxane, followed by intramolecular cyclization under basic conditions gave BFP **13c**. Compound **13g** was prepared by reductive amination of compound **13c**. Compounds **13a**, **13c–f**, **13h–j**, and **14–17** were prepared in a similar fashion using common intermediate 11 and commercially available *N*-Boc-protected aminoacids.[9]

While a majority of the C-linked cyclic and acyclic analogs showed potent activity against CDC7, several compounds (**13b**, **13f**, and **13i**) also emerged with enhanced selectivity over PIM and CK2 (Table 3). Despite potent biochemical activity for **13f**, this compound only showed modest cellular potency (pMCM2 IC_{50} = 874 nM). In contrast, both **13b** and **13i** demonstrated cell

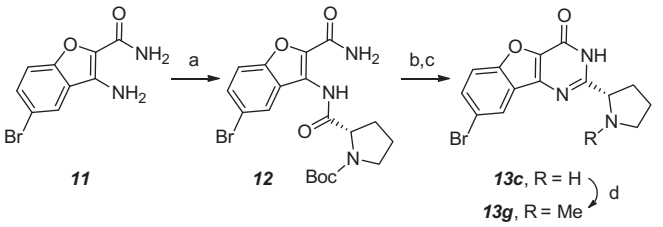

Scheme 2. Reagents and conditions: (a) *N*-Boc-proline, cyanuric chloride, DMA, 0 °C → rt, 90%; (b) 4NHCl, dioxane, ~100%; (c) NaOH, EtOH, 85 °C, 95%; (d) $(CH_2O)_n$, $Na(CN)BH_3$, DMA.

Table 2
N-linked pyrrolidine analogs[10,11]

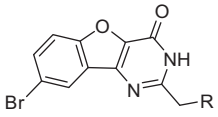

	R =		
3	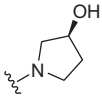	CDC7 CK2 PIM1 pMCM2	7.7 28 11 1471
10a	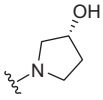	CDC7 CK2 PIM1 pMCM2	5.5 89 13 1805
10b	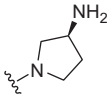	CDC7 CK2 PIM1 pMCM2	10 70 3.8 625
10c	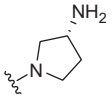	CDC7 CK2 PIM1 pMCM2	207 535 6.0 —
10d		CDC7 CK2 PIM1 pMCM2	3.7 92 13 353
10e	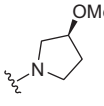	CDC7 CK2 PIM1 pMCM2	11 512 77 362
10f	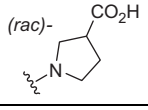	CDC7 CK2 PIM1 pMCM2	13 49 142 >40,000

Table 3
C-linked Analogs[10,11]

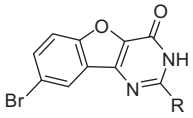

	R =		
13a		CDC7 CK2 PIM1 pMCM2	7.7 43 18 2536
13b		CDC7 CK2 PIM1 pMCM2	4.8 91 31 75
13c		CDC7 CK2 PIM1 pMCM2	70 1506 104 4592
13d	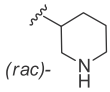	CDC7 CK2 PIM1 pMCM2	15 175 39 2356
13e	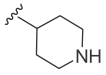	CDC7 CK2 PIM1 pMCM2	6.2 50 22 1434
13f	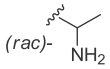	CDC7 CK2 PIM1 pMCM2	7.9 757 72 874
13g		CDC7 CK2 PIM1 pMCM2	7.3 63 11 802
13h	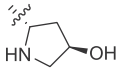	CDC7 CK2 PIM1 pMCM2	9.1 418 73 440
13i	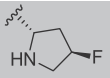	CDC7 CK2 PIM1 pMCM2	3.7 238 46 82
13j	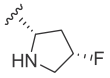	CDC7 CK2 PIM1 pMCM2	11 3618 11 566

potencies below 100 nM in the pMCM2 cell-based assay, and thus were considered as optimal substituents for the right hand side. In addition to the improved selectivity versus PIM1 and CK2, these two analogs also demonstrated good plasma exposures in mouse PK studies dosed at 100 mg/kg (PO) (**13b**: 195 μM, 1 h; 71 μM, 4 h; 13i: 82 μM, 1 h; 46 μM, 4 h).

With the right-hand side optimized, we went back to survey the left-hand side with the right fixed as either the (*S*)-pyrrolidin-2-yl- or the (2*S*,4*R*)-4-fluoropyrrolidin-2-yl- substituted (Table 4). We found that replacement of the 8-bromo with either the 8-chloro or the 8-methoxy group resulted in further improvements to the selectivity profile in both series, especially against CK2. The 8-methoxy substituted analogs (**16** and **17**) were less potent in cell assay than the 8-bromo analogs (**13b** and **13i**). In addition, the 8-chloro analogs (**14** and **15**), were more selective for CDC7. Overall, the replacement of bromine in the 8-position of BFP core with chlorine, and (*S*)-pyrrolidin-2-yl as a right hand side substituent in **14** led to the best combination in terms of selectivity profile (>60-fold selectivity against CK2, >10-fold selectivity against PIM, and >300-fold selectivity against a panel of over 100 protein kinases) and improved cell based potency (pMCM2 MDA-MB-231T IC_{50} = 118 nM, and Colo-205 IC_{50} = 140 nM). Compound **14** demonstrated excellent plasma exposures in mice [100 mg/kg (PO): 141 μM (1 h), 81 μM (4 h)], and possessed the best PK properties among compounds in Table 4. Overall, compound **14** met our target property profile and was selected for further characterization.

The biochemical potency of **14** translates into inhibition of CDC7 specific phosphorylation of MCM2 in cells cell lines that over express CDC7 and phosphorylated MCM2 (data shown for MDA-MB-231T and Colo-205 cell lines). In addition, flow cytometry analysis of Colo-205 cells treated with 14 causes dose-dependent accumulation of cells in the late S and G2 phases of the cell cycle, consistent with impaired DNA synthesis (Figure ure3). Similar results were found in 27 of 31 tumor cell lines that were tested (results not shown). Prolonged treatment with compound **14** (3 days) inhibited the cell proliferation (IC_{50} = 2685 nM), decreased cell viability (IC_{50} = 2142 nM) and elicited the caspase 3/7 activity (EC_{50} = 2288 nM) in Colo-205 cells.[11] Profound proliferation reduction was also observed in a variety of tumor lines tested (data not shown). In addition, compound **14** also significantly inhibited the

Table 4
The replacement of bromine in **13b** and **13i**[10,11]

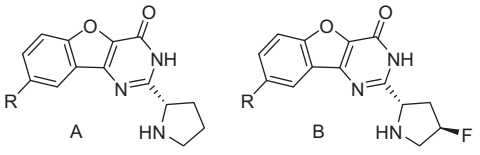

R	A	IC_{50} (nM)		B	IC_{50} (nM)	
Br	**13b**	CDC7	4.8	**13i**	CDC7	3.7
		CK2	91		CK2	238
		PIM1	31		PIM1	46
		pMCM2	75		pMCM2	82
Cl	**14**	CDC7	3.4	**15**	CDC7	4.0
		CK2	215		CK2	752
		PIM1	42		PIM1	65
		pMCM2	118		pMCM2	167
MeO	**16**	CDC7	6.1	**17**	CDC7	3.9
		CK2	238		CK2	733
		PIM1	77		PIM1	102
		pMCM2	1374		pMCM2	292

Data shown for pMCM in MDA-MB-231T cell line.

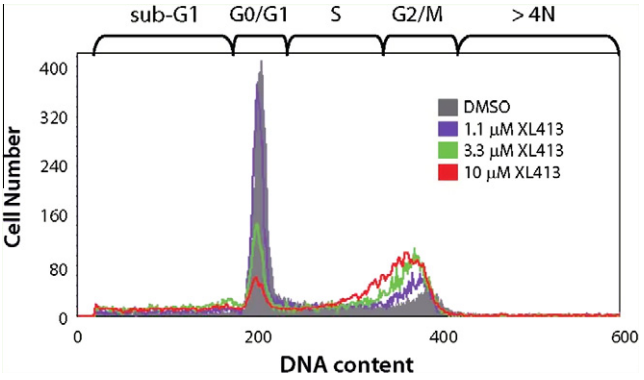

Figure 3. Flow cytometry analysis of Colo-205 cells treated with **14** (XL413). Colo-205 cells were treated for 24 h with 1.1, 3.3, or 10 μM of compound **14** and analyzed for DNA content using propidium iodide.

anchorage-independent growth of colo-205 in soft agar (IC_{50} = 715 nM). Collectively, the cell data is consistent with the literature evidence that inhibiting CDC7 results in modified S phase progression that subsequently leads to apoptotic cell death.[3]

Compound **14** demonstrated an excellent exposure profile in full rat PK assay (dosed at 3 mg/kg: C_{max} (PO) = 8.61 μM, AUC (po) = 75 μM h, CL = 117 mL/h kg, V_{ss} = 0.55 L/kg, $T_{1/2}$ = 2.32 h, F = 95%). This translated into robust activity in in vivo pharmacodynamic studies. In a Colo-205 xenograft model, dose dependent target modulation was observed (Fig. 4); and a 70% inhibition of phosphorylated MCM2 was detected even at the 3 mg/kg dose. The ED_{50} is calculated to be <3 mg/kg.

Multiple-dose studies of **14** in a Colo-205 xenograft model demonstrates significant anti-tumor efficacy. Tumor bearing mice were administered **14** orally at doses of 10, 30, or 100 mg/kg once daily (qd) for 14 days (Fig. 5). Two alternate dosing regimens were also examined in this study: a dose of 30 mg/kg administered twice-daily (bid) and a dose of 100 mg/kg administered every-other day (q2d). Compound **14** was well tolerated at all the doses and regimens examined, with no significant body weight loss observed. Only modest tumor growth inhibition (36%) was observed for the 10 mg/kg qd dosage, but significant tumor growth inhibition (83%) was observed at the 30 mg/kg qd dose. More impressively, significant tumor growth regression (32%) was observed if dosed twice-daily at 30 mg/kg. The ED_{50} is estimated at 13 mg/kg.

In this paper we report the discovery of XL413 (compound **14**), a potent and selective ATP competitive CDC7 inhibitor. XL413 is a novel benzofuropyrimidinone CDC7 inhibitor with a very favorable pharmacokinetic profile and demonstrates significant tumor growth regression in rodent models. XL413's tumor growth regression is linked to the arrest of tumor cells in the late S to G2 phase of

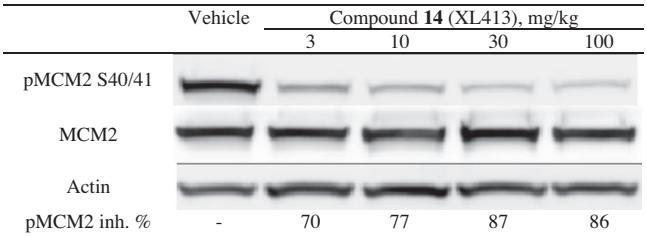

Figure 4. Pharmacodynamic dose response of **14** (XL413) in a Colo-205 xenograft model. Athymic nude mice bearing Colo-205 xenograft tumors were dosed orally with 3, 10, 30, and 100 mg/kg of **14**. Plasma and tissue samples were taken at 4 h post-dose and analyzed for levels of phosphorylated MCM2 and MCM2 by Western immunoblot analysis.

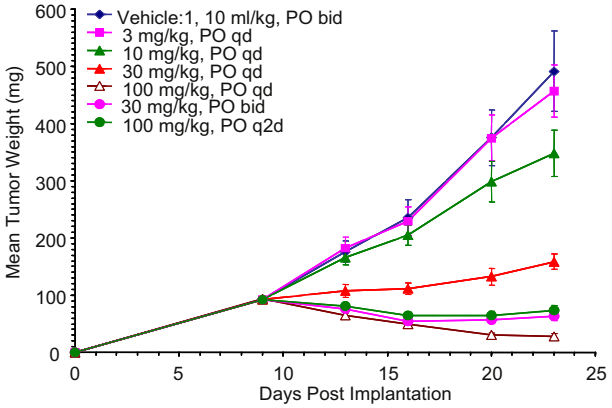

	TGI (%)	Regression (%)	BW loss (%)	Dose skips
3 mg/kg qd	8.7 (ns)		-0.5	1
10 mg/kg qd	36 (ns)		-3.4	1
30 mg/kg qd	83		-8.3	5
100 mg/kg qd	>100	70	-4.7	7
30 mg/kg bid	>100	32	-6.4	6
100 mg/kg q2d	>100	21	-4.5	5

Figure 5. Colo-205 nude mouse xenograft study with **14** (XL413).

the cell cycle, a cell phenotype indicative of CDC7 inhibition. In addition, XL413 is relatively CYP clean (CYP3A4, 2C9, 2D6, 2C19 IC_{50} >50 μM, CYP1A2 IC_{50} = 6.9 μM) among the major isoforms tested; and was inactive against hERG (IC_{50} > 30 μM). The attractive profile of XL413 resulted in its selection for preclinical development and subsequent advancement into Phase 1 clinical trials.

Acknowledgments

The authors greatly appreciate contributions from Jason Chew, Leanne Goon, Stuart Johnson, Eun Ok Kim, Iris Ngan, Yongchang Shi, Scott Detmer, Richard Venture, Rui Lin, Nicole Miller, Tim Heuer, Douglas Den Otter and the departments of Exelixis Genome Biochemistry, New Lead Discovery, Cell facility, and Compound Repository.

References and notes

1. For general reviews see: (a) Sawa, M.; Masai, H. *Drug Des. Dev. Ther.* **2008**, *2*, 255; (b) Montagnoli, A.; Moll, J.; Colotta, F. *Clin. Cancer Res.* **2010**, *16*, 4503.
2. (a) Hartwell, L. H. *J. Mol. Biol.* **1976**, *104*(4), 803; (b) Patterson, M.; Sclafani, R. A.; Fangman, W. L. *Mol. Cell Biol.* **1986**, *276*, 1376; (c) Sclafani, R. A. *J. Cell Sci.* **2000**, *13*, 2111; (d) Snaith, H. A.; Brown, G. W.; Forburg, S. L. *Mol. Cell Biol.* **2000**, *20*, 7922; (e) Takeda, T.; Ogino, K.; Tatebayashi, K.; Ikeda, H.; Akai, Ki.; Masai, H. *Mol. Biol. Cell* **2001**, *12*, 1257; (f) Fung, A. D.; Ou, J.; Bueler, S.; Brown, G. W. *Mol. Cell Biol.* **2002**, *22*, 4477; (g) Matsumoto, S.; Ogino, K.; Noguchi, E.; Russell, P.; Masai, H. *J. Biol. Chem.* **2005**, *280*, 42536; (h) Sommariva, E.; Pellny, T. K.; Karahan, N.; Kumar, S.; Huberman, J. A.; Dalgaard, J. Z. *Mol. Cell Biol.* **2005**, *25*, 2770; (i) Montagnoli, A.; Moll, J.; Colotta, F. *Clin. Cancer Res.* **2010**, *16*, 4503.
3. (a) Montagnoli, A.; Tenca, P.; Sola, F.; Carpani, D.; Brotherton, D.; Albanese, C.; Santocanale, C. *Cancer Res.* **2004**, *64*, 7110; (b) Kim, J. M.; Kakusho, N.; Yamada, M.; Kanoh, Y.; Takemoto, N.; Masai, H. *Oncogene* **2008**, *27*, 3475.
4. Bonte, D.; Lindvall, C.; Liu, H.; Dykema, K.; Furge, K.; Weinreich, M. *Neoplasia* **2008**, *10*, 920.
5. (a) Menichincheri, M.; Albanese, C.; Alli, C.; Ballinari, D.; Bargiotti, A.; Caldarelli, M.; Ciavolella, A.; Cirla, A.; Colombo, M.; Colotta, F.; Croci, V.; D'Alessio, R.; D'Anello, M.; Ermoli, A.; Fiorentini, F.; Forte, B.; Galvani, A.; Giordano, P.; Isacchi, A.; Martina, K.; Molinari, A.; Moll, J. K.; Montagnoli, A.; Orsini, P.; Orzi, F.; Pesenti, E.; Pillan, A.; Roletto, F.; Scolaro, A.; Tatò, M.; Tibolla, M.; Valsasina, B.; Varasi, M.; Vianello, P.; Volpi, D.; Santocanale, C.; Vanotti, E. *J. Med. Chem.* **2010**, *53*, 7296; (b) Menichincheri, M.; Bargiotti, A.; Berthelsen, J.; Bertrand, J. A.; Bossi, R.; Ciavolella, A.; Cirla, A.; Cristiani, C.; Croci, V.; D'Alessio, R.; Fasolini, M.; Fiorentini, F.; Forte, B.; Isacchi, A.; Martina, K.; Molinari, A.; Montagnoli, A.; Orsini, P.; Orzi, F.; Pesenti, E.; Pezzetta, D.; Pillan, A.; Poggesi, I.; Roletto, F.; Scolaro, A.; Tato, M.; Tibolla, M.; Valsasina, B.; Varasi, M.; Volpi, D.; Santocanale, C.; Vanotti, E. *J. Med. Chem.* **2009**, *52*, 293; (c) Zhao, C.; Tovar, C.; Yin, X.; Xu, Q.; Todorov, I. T.; Vassilev, L. T.; Chen, L. *Bioorg. Med. Chem. Lett.* **2009**, *19*, 319; (d) Vanotti, E.; Amici, R.; Bargiotti, A.; Barthelsen, J.; Bosotti, R.; Ciavolella, A.; Cirla, A.; Cristiani, C.; D'Alessio, R.; Forte, B.; Isacchi, A.; Martina, K.; Molinari, A.; Menichincheri, M.; Montagnoli, A.; Orsini, P.; Pillan, A.; Roletto, F.; Scolaro, A.; Tibolla, M.; Valsasina, B.; Varasi, M.; Volpi, D.; Santocanale, C. *J. Med. Chem.* **2008**, *51*, 486; (e) Shafer, C. M.; Lindvall, M.; Bellamacina, C.; Gesner, T. G.; Yabannavar, A.; Jia, W.; Lin, S.; Walter, A. *Bioorg. Med. Chem. Lett.* **2008**, *18*, 4482.
6. Tsuhako, A.L.; Brown, D.S.; Koltun, E.S.; Aay, A.; Arcalas, A.; Chan, V.; Du, H.; Engst, S.; Franzini, F.; Galan, A.; Huang, P.; Johnston, S.; Kane, B.; Kim, M.H.; Stott, G.; Stout, T.J.; Yu, P.;Zaharia, Z.A.; Zhang, W.; Zhou, P.; Nuss, J.M.; Kearney, P.C.; Xu, W. *Bioorg. Med. Chem. Lett.* **2012.** http://dx.doi.org/10.1016/j.bmcl.2012.04.025.
7. The CDC7 homology model was built using MOE 2009 (Chemical Computing Group, Inc.).
8. (a) Niefind, K.; Guerra, B.; Ermakowa, I.; Issinger, O. *EMBO J.* **2001**, *20*, 5320; (b) Niefind, K.; Guerra, B.; Pinna, L.; Issinger, O.; Schomburg, D. *EMBO J* **1998**, *17*, 2451. The X-ray crystal structure coordinates of **3** in CK2 have been deposited in the Protein Data Bank (PDB code 4ANM).
9. Detailed experimentals for this manuscript can be found in the following patent: Brown, S. D.; Du, H.; Franzini, M.; Galan, A. A.; Huang, P.; Kearney, P.C.; Kim, M. H.; Koltun, E. S.; Richards, S. J.; Tsuhako, A.L.; Zaharia, C.A. WO 2009086264 A1 2009.
10. Biochemical assay: N-terminally Myc-tagged human CDC7 (amino acids: E2–L574) and N-terminally His-tagged human ASK (N2–F674) were co-expressed in *E. coli* and purified using nickel affinity chromatography. Human CK2 α isoform A (R8–R333) and full-length β subunits were expressed separately as N-terminally MBP-tagged proteins in *E. coli* and purified using amylose Sepharose chromatography. The purified subunits were reconstituted to form the tetrameric α2β2 CK2 holoenzyme. Human PIM1 (E32–D292) was expressed as N-terminally His-tagged proteins in *E. coli* and purified using nickel affinity chromatography. Protein concentration was determined by the Bradford assay and identification was confirmed by trypsin digestion and mass spectrometry. Kinase activity and compound inhibition were determined using the luciferase-luciferin-coupled chemiluminescence assay and measured as the percentage of ATP utilized following the kinase reaction in a 384-well format as described previously The final CDC7 kinase assay condition was 6 nM CDC7/ASK, 1 μM ATP, 50 mM Hepes pH 7.4, 10 mM $MgCl_2$, 0.02% BSA, 0.02% brij 35, 0.02% tween 20 and 1 mM DTT. It is worthy to note that the CDC7/ASK protein exhibited substrate-independent ATP utilization. The final PIM1 kinase assay condition was 2.4 nM PIM1, 0.5 μM ATP, 10 μM peptide substrate (AKRRRLSA), 20 mM Hepes pH 7.4, 10 mM $MgCl_2$, 0.03% Triton, and 1 mM DTT. The final CK2 kinase assay condition was 4 nM CK2 holoenzyme, 2 μM ATP, 2 μM casein, 20 mM Hepes pH 7.5 10 mM $MgCl_2$, 0.03% Triton, 1 mM DTT and 0.1 mM $NaVO_3$. All kinase reactions were incubated at room temperature for 1–2 h. Munagala, N. Nguyen S., Lam W., Lee J., Joly A., McMillan K. and Zhang W. Assay Drug Dev Technol., 2007, 5, 65–73.
11. Cell assays: Endogenous MCM2 phosphorylation fixed cell immunofluorescence assay was conducted with MDA-MB-231T cells (from ATCC) seeded at 1.0×10^4 cells/well onto 96-well plates in complete DMEM containing 10% FBS. Cells were treated serial dilutions of test compound in 3% DMSO and incubated for 4 h. Cells were then fixed for 20 min treated with Triton X-100 in PBS for 5 min, followed by overnight incubation with pMCM2 (S53) antibody (#AN3011, custom produced for Exelixis by Anaspec, Inc.). pMCM2 (S53) was read on a Cellomics Arrayscan after incubation with Alexa Fluor 546 Goat anti-rabbit IgG (H+L) (Cat#A11010, Invitrogen). IC_{50} values were determined based on pMCM2 (S53) intensity with compound treatment versus pMCM2 (S53) intensity with DMSO treatment alone. The cell proliferation was measured by BrdU incorporation assay, viability was assayed by Cell Titer–Glo kits, and the apoptosis assay was measured by Apo-ONE Homogeneous Caspase-3/7 Assay kit (Promega).